Molecular BioSystems

RSC Publishing

PAPER

View Article Online
View Journal

Cite this: DOI: 10.1039/c3mb70213h

Role of feedback and network architecture in controlling virulence gene expression in *Bordetella*†

Mahendra Kumar Prajapat and Supreet Saini*

Received 5th June 2013,
Accepted 27th August 2013

DOI: 10.1039/c3mb70213h

www.rsc.org/molecularbiosystems

Bordetella is a Gram-negative bacterium responsible for causing whooping cough in a broad range of host organisms. For successful infection, *Bordetella* controls expression of four distinct classes of genes (referred to as class 1, 2, 3, and 4 genes) at distinct times in the infection cycle. This control is executed by a single two-component system, BvgAS. Interestingly, the transmembrane component of the two-component system, BvgS, consists of three phospho-transfer domains leading to phosphorylation of the response regulator, BvgA. Phosphorylated BvgA then controls expression of virulence genes and also controls *bvgAS* transcription. In this work, we perform simulations to characterize the role of the network architecture in governing gene expression in *Bordetella*. Our results show that the wild-type network is locally optimal for controlling the timing of expression of the different classes of genes involved in infection. In addition, the interplay between environmental signals and positive feedback aids the bacterium identify precise conditions for and control expression of virulence genes.

Introduction

Bordetella is a Gram-negative coccobacillus that colonizes the respiratory tracts of mammals.[1,2] *B. pertussis*, *B. parapertussis*, and *B. bronchiseptica* are closely related subspecies and are pathogenic in a variety of hosts.[3–5] Among these, *B. pertussis* is exclusively adapted to humans[6] with no known other animal or environmental hosts, and is a causative agent of the highly contagious acute respiratory disease whooping cough or pertussis.[7] Transmission of *B. pertussis* occurs *via* respiratory droplets and environmental contamination with respiratory secretions.[1,8,9] Among the different sub-species, differences exist regarding the virulence genes encoded on the genome.

Bordetella employs a number of strategies to survive and cause infection in the host. These involve expression of virulence factors expressed at different stages of infection, and include factors responsible for colonization and toxemia.[10,11] The initial catarrhal phase begins with mild cold-like symptoms when the bacterium colonizes ciliated epithelial cells of the upper respiratory tract.[11,12] The evolvement to the paroxysmal phase is characterized by intense coughing bursts that are often followed by immense aspiratory effort that sounds like ''whoop''.[11,13,14]

Virulence factors responsible for infection are encoded by a large number of genes encoded at various locations in the chromosome. Interestingly, expression of all virulence genes is known to be regulated in *Bordetella* by a single two-component phosphor-transduction system called BvgAS. Although the precise environmental cues that trigger the BvgAS system active or inactive are not well understood, in a laboratory setting, expression of virulence genes is induced by growth at 37 °C in the absence of $MgSO_4$ and nicotinic acids.[15,16] Similarly, BvgAS-induced genes are repressed in the laboratory by growth at lower temperatures, and addition of $MgSO_4$ and nicotinic acid.[15–17] Further, BvgAS regulated genes show three different phenotypic phases in *Bordetella*, classified as Bvg^-, Bvg^i and Bvg^+.[1,18,19] These are classified on the basis of the strength of external signals in inducing BvgAS phosphorylation, and subsequent activation of downstream genes.

In the presence of signals leading to activation of the BvgAS system, the auto-kinase domain of BvgS autophosphorylates and transfers the phosphate in a three-step phosphorelay (Fig. 1). Phosphorylated BvgA differentially regulates virulence genes associated with pathogenesis in *Bordetella.*[18,20,21] The virulence genes are classified into four classes according to the binding affinity of their promoters to phosphorylated BvgA and phenotypic expression.[18,20] The promoters of *flaA*, *frlA* and *frlB* (all three related to motility) are repressed by phosphorylated BvgA,[22–24] and are classified as class 1 promoters.[23] Their precise role in pathogenesis is not well understood. The promoter for *bipA* has both high-affinity binding sites upstream

Department of Chemical Engineering, Indian Institute of Technology Bombay, Powai, Mumbai - 400076, Maharashtra, India. E-mail: saini@che.iitb.ac.in; Tel: +91-22-2576-7216

† Electronic supplementary information (ESI) available. See DOI: 10.1039/c3mb70213h

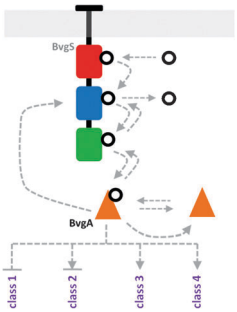

Fig. 1 Cartoon representation of the BvgAS regulatory network. In simulating conditions, BvgS autophosphorylates itself, and passes the phosphate group (black circles) to BvgA (triangle) in three steps. Phosphorylated BvgA then controls expression of class 1, 2, 3, and 4 genes. In addition, BvgA-P also controls expression of BvgA and BvgS. The three domains of BvgS are autokinase (red), receiver (blue), and phosphotransfer (green) domains. Phosphorylated BvgA regulates expression of class 1, 2, 3, and 4 genes *via* transcription control as shown in the figure. In addition, phosphorylated BvgA positively regulates expression of BvgA and BvgS. This positive feedback is represented by the two curved arrows from BvgA-P (triangle with a black ring) to BvgA (triangle) and BvgS.

of the *bipA* transcription start site and low-affinity binding sites downstream of the *bipA* transcription start site.[25,26] This results in repression of BipA expression in Bvg^- (when both binding sites are unoccupied) and Bvg^+ (when both sites are occupied) phases, but expression in the Bvg^i phase (when only the high affinity site is occupied).[27,28] The *bipA* promoter is classified as belonging to class 2. The promoters for *fhaB*,[29] *fim2*,[30] *prn*[31] and *tcfA*[12] contain high-affinity binding sites for phosphorylated BvgA[20,32,33] and are classified as under the control of class 3 promoters. The promoters for *cyaA*,[34] *ptxA*,[35] *bsc* locus,[36,37] *dnt*[38,39] and *pagP*[40] contain low-affinity BvgA binding sites; therefore they are expressed late in the Bvg^+ phase.[20,21,32] The promoters of these genes are grouped together as class 4 promoters.

While the mechanistic details of the phosphorelay system are beginning to be understood, not much is known about the dynamics and control of gene expression in the *Bordetella* phosphorelay system.[18,20,27,28,33,41,42] In addition, how a particular network structure (Fig. 1) aids the bacterium in effectively controlling gene expression of four distinct gene classes is not well understood. To answer this question, we formulated a stochastic mathematical model of phosphorelay control of virulence gene expression at a single-cell resolution. Using the model, we deconstruct the network in a piecewise manner, and elucidate the role of each interaction in dictating gene expression dynamics. Specifically, we investigate the role of multiple feedback loops encoded in the system, and analyze their impact on gene expression. Our results help understand how BvgAS topology is locally optimal in the parameter space for gene expression control in *B. pertussis*, and identify kinetic parameters critical for its optimum function. We also demonstrate that the bacterium combines environmental signals and the positive-feedback strength to recognize precise environmental conditions and appropriately tune gene expression.

Model construction

Model description and assumptions

The model captures the biochemical and genetic interactions in the BvgAS regulatory network using the algorithm proposed by Gillespie.[43,44] The following interactions are captured in the model: (a) auto-phosphorylation of BvgS in response to environmental signals; (b) phosphor-transduction leading to phosphorylation of BvgA; (c) binding of phosphorylated BvgA at virulence gene promoters; (d) feed-forward negative control at the aspartic acid domain by dephosphorylation; (e) transfer of phosphate from BvgA to BvgS; (f) BvgA-controlled positive feedback loop in the network; and (g) degradation terms for all species of BvgS, BvgA, and the various classes of genes. Each simulation was carried out for 1000 cells, and the results were then analyzed both at a population average level and at a single-cell resolution. In all, six transitions between the three environmental conditions were studied. These are enumerated as (a) Bvg-repressing (Bvg^-) to Bvg-intermediate (Bvg^i); (b) Bvg^i to Bvg-activating (Bvg^+); (c) Bvg^- to Bvg^+; (d) Bvg^i to Bvg^-; (e) Bvg^+ to Bvg^i; and (f) Bvg^+ to Bvg^-.

The major assumptions that have been used in formulating the model described in this work are as enumerated below:

(1) In designing this model, we focus solely on the BvgAS phosphorelay system and its role in regulating the expression of four classes of virulence genes in *Bordetella*. The role of any other regulatory signal or protein has not been included.

(2) Transcription and translation are lumped together in the model, and are not treated separately. There is considerable evidence that the BvgAS system in *B. pertussis* is primarily regulated at the transcription level.[21,45,46] In addition, mRNA half lives have been shown to be considerably longer than other time scales in the system, and hence, are not likely to be the most important factors in determining the dynamics of the system.

(3) BvgS has been assumed as a polydomain protein consisting of three domains, namely, the N-terminal histidine autokinase domain (transmitter), the aspartic acid domain (receiver), and the C-terminal histidine domain. Hence, in the dynamics of the model, we track concentration of four BvgS species: unphosphorylated BvgS, BvgS-P1 (phosphorylated autokinase domain), BvgS-P2 (phosphorylated aspartic acid domain) and BvgS-P3 (phosphorylated histidine domain).[47]

(4) Similarly, two species of BvgA have been considered to coexist: the unphosphorylated BvgA and BvgA-P. BvgA-P is the phosphorylated form that regulates the transcription of virulence genes of four classes.[45,47,48]

(5) An environmental signal (S) has been assumed which triggers BvgS auto-phosphorylation.[49] The strength of the environmental signal is accounted for in the model by varying the numerical values assigned to the variable S. The S values represent the Bvg^- (at low value, $S = 0$), Bvg^i (at intermediate value, $S = 1.5$), and Bvg^+ (at high value, $S = 9$) phases.

(6) The *bvgAS* promoter was assumed to contain two distinct promoters: one which is activated by the phosphorylated BvgA, and the other which is activated weakly by factors other than BvgA.

(7) For modeling the mutant gene expression, all biochemical and kinetic parameters in the model were kept the same as those in the wild type. For modeling mutants, the appropriate parameters were changed to another appropriate value.

(8) Phosphorylated BvgA is known to be stable in a dimeric form. Hence, in our model, we have assumed that transcription of the virulence genes is controlled by phosphorylated BvgA in the dimer form.[50–52]

Model equations

With the above-listed assumptions, we formulated the kinetic model as shown below. Since the model is stochastic in nature, at each time step it estimates relative probabilities of each reaction taking place (listed below). A reaction takes place at each time step based on the probabilities and the ''concentrations'' are accordingly updated. A new set of probabilities are then generated for the next time step. There are insufficient experimental data to uniquely estimate the parameters associated with the model. Hence, we chose parameter values to best represent the available experimental data qualitatively. After choosing the values of the parameters (Table 1), we tested the uniqueness of the parameter values by running a genetic algorithm on randomized parameter values and observing their convergence as the error between the model output and the experimental values was minimized (data not shown). The kinetic profiles generated by the model were tested against the available data.

Table 1 List of parameters used in the model

Parameter	Value[a,b]
k_1	2.0
k_{1a}	10.0
k_{1b}	5.0
k_2	15.0
k_3	1.6
k_4	15.0
k_5	1.7
k_6	2.0
k_{6p}	0.5
k_{6q}	0.5
k_7	1.0
k_{7r}	0.5
k_{7s}	0.5
k_8	0.01
k_9	0.01
k_{10}	0.025
k_{11}	4.0
k_{11a}	1.5
k_{12}	1.0
k_{12r}	0.55
k_{13}	12
k_{13r}	4.5
k_{13a}	1.8
k_{14}	5.0
k_{14a}	0.1
k_{15}	6.5
k_{15a}	10.0
k_{16}	0.05
k_{17}	0.06
k_{18}	0.09
k_{19}	0.09
k_{20}	0.1

[a] All degradation rates are represented in h^{-1} units. [b] We are unable to represent the kinetic parameters in dimensions. Hence, they are presented here in a dimensionless concentration unit.

Auto-phosphorylation of BvgS into BvgS-P1

$$r_1 = \frac{(k_1 \times \mathrm{BvgS} \times S/k_{1a})}{(1 + S/k_{1a}) \times (k_{1b} + \mathrm{BvgS})} \quad (1)$$

Transfer from BvgS-P1 to BvgS-P2

$$r_2 = k_2 \times \mathrm{BvgS\text{-}P1} \quad (2)$$

Transfer from BvgS-P2 to null

$$r_3 = k_3 \times \mathrm{BvgS\text{-}P2} \quad (3)$$

Transfer from BvgS-P2 to BvgS-P3

$$r_4 = k_4 \times \mathrm{BvgS\text{-}P2} \quad (4)$$

Transfer from BvgS-P3 to BvgS-P2

$$r_5 = k_5 \times \mathrm{BvgS\text{-}P3} \quad (5)$$

Transfer from BvgS-P3 to BvgA

$$r_6 = \frac{(k_6 \times \mathrm{BvgS\text{-}P3} \times \mathrm{BvgA})}{(k_{6p} + \mathrm{BvgS\text{-}P3}) \times (k_{6q} + \mathrm{BvgA})} \quad (6)$$

Transfer from BvgA to BvgS-P3

$$r_7 = \frac{(k_7 \times \mathrm{BvgA\text{-}P} \times \mathrm{BvgS})}{(k_{7r} + \mathrm{BvgS}) \times (k_{7s} + \mathrm{BvgA\text{-}P})} \quad (7)$$

Degradation of BvgS

$$r_8 = k_8 \times \mathrm{BvgS} \quad (8)$$

Degradation of BvgA

$$r_9 = k_9 \times \mathrm{BvgA} \quad (9)$$

Degradation of BvgA-P

$$r_{10} = k_{10} \times \mathrm{BvgA\text{-}P} \quad (10)$$

BvgA-P activates BvgAS

$$r_{11} = \frac{k_{11} \times (\mathrm{BvgA\text{-}P})^2}{\left[(k_{11a})^2 + (\mathrm{BvgA\text{-}P})^2\right]} \quad (11)$$

BvgA-P represses class 1

$$r_{12} = \frac{k_{12}}{\left[1 + (\mathrm{BvgA\text{-}P}/k_{12r})^2\right]} \quad (12)$$

BvgA-P activates and then represses class 2

$$r_{13} = \frac{k_{13} \times (\mathrm{BvgA\text{-}P})^2}{\left[(k_{13a})^2 + (\mathrm{BvgA\text{-}P})^2\right] \times \left[1 + (\mathrm{BvgA\text{-}P}/k_{13r})^2\right]} \quad (13)$$

BvgA-P activates class 3

$$r_{14} = \frac{k_{14} \times (\mathrm{BvgA\text{-}P})^2}{\left[(k_{14a})^2 + (\mathrm{BvgA\text{-}P})^2\right]} \quad (14)$$

BvgA-P activates class 4

$$r_{15} = \frac{k_{15} \times (\text{BvgA-P})^4}{\left[(k_{15a})^4 + (\text{BvgA-P})^4\right]} \quad (15)$$

Degradation of class 1

$$r_{16} = k_{16} \times \text{class 1} \quad (16)$$

Degradation of class 2

$$r_{17} = k_{17} \times \text{class 2} \quad (17)$$

Degradation of class 3

$$r_{18} = k_{18} \times \text{class 3} \quad (18)$$

Degradation of class 4

$$r_{19} = k_{19} \times \text{class 4} \quad (19)$$

BvgA-independent (basal) production of BvgAS

$$r_{20} = k_{20} \quad (20)$$

Sensitivity analysis

Sensitivity analysis was performed on 200 cells. The sensitivity of the steady-state behaviour to all parameters used in the model was tested by perturbing the parameter values, and computing the new steady state values. For each parameter, the new values assigned ranged from 0 to two times the parameter value used in the model. Variation in steady state values was computed for each class of genes in the ''off'' to ''on'' as well as ''on'' to ''off'' transitions.

Results and discussion

Bordetella controls expression of four classes of genes involved in pathogenesis

Bordetella, in order to cause a successful infection, must express genes from four distinct classes (classified as class 1, 2, 3, and 4) at different times of the infection cycle.[33,53–57] As a first step towards understanding the role of the three-step phospho-relay system encoded in the BvgAS two-component system, we modelled the gene expression dynamics in wild-type *Bordetella*, and studied the transition between Bvg-inducing conditions (Bvg^+), Bvg-intermediate conditions (Bvg^i), and Bvg-repressing conditions (Bvg^-).[1,18,19] As detailed in the methods section, the simulations were carried out using the Gillespie algorithm for stochastic reactions.[43,44] The simulations were carried out for 1000 cells, and the average data are reported.

We note that our data are able to capture the previously reported experimentally observed dynamics of gene expression[18,20,28,41] (Fig. 2). As cells transition from Bvg^- to Bvg^+ conditions, class 1 genes (flagella genes) are repressed. In addition, class 2 genes demonstrate a biphasic behavior where they are activated at intermediate values of BvgA-P, but repressed at higher values of the activator.[25–28] Class 3 and class 4 genes are activated as cells transition from Bvg^- to Bvg^+. Their transition is consistent with

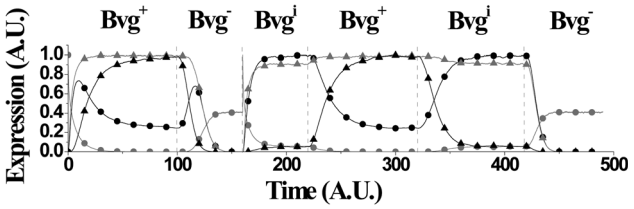

Fig. 2 Normalized wild-type gene expression dynamics of class 1 (grey circles), class 2 (black circles), class 3 (grey triangles), and class 4 (black triangles) under various environmental conditions. The graph captures dynamics in wild-type *Bordetella* in the six possible transitions between Bvg^-, Bvg^i, and Bvg^+ conditions. The transitions were studied by varying the environmental signal strength, *S*, as outlined in the methods section.

previous reports where BvgA-P has a greater affinity for class 3 promoters as compared to class 4 promoters, leading to a difference in their dynamics of activation.[20,32] This difference is captured in our simulation results in Fig. 2.

Fig. 2 also highlights the salient features of dynamics of gene expression as cells transition from one phase to another. Specifically, as cells move from Bvg^- to Bvg^i conditions, the repression of class 2 genes at high levels of BvgA-P is abolished, and we only observe a monotonic increase in class 2 gene expression. Also, in this transition (Bvg^- to Bvg^i), class 4 gene expression is minimal (consistent with its promoters binding weakly to BvgA-P) whereas class 3 gene expression is about 60–70% of its fully induced levels, consistent with previously published reports.[20,28,41]

As cells transition from Bvg^+ to Bvg^i or from Bvg^+ to Bvg^-, the reverse is observed. Dynamically, class 3 gene expression is repressed at a later time compared to class 4, while class 1 genes are induced from near-zero expression values. On transition from Bvg^+ to Bvg^i, consistent with our understanding of the system, while class 4 genes are repressed significantly (about 90%), there is only about 25% reduction in the expression of class 3 genes[20,28,41] (Fig. 2).

Thus, we observe that our model is able to semi-quantitatively explain the dynamics of gene expression in *B. pertussis*. However, our aim is to understand and characterize the advantages that the complex BvgAS phospho-relay system confers to the organism as compared to the two-component systems ubiquitous in bacteria.[58] To investigate this further, we performed a piecewise deconstruction of the BvgAS system, and studied the impact on the dynamics of gene expression in the four classes involved in pathogenesis.

Presence of three phospho-transfer domains in BvgS confers flexibility to the response of the bacterium to environmental fluctuations

The distinguishing feature of BvgS from many other transmembrane proteins is the presence of three phospho-transfer domains (namely the autokinase, receiver, and the phosphotransfer domains) (Fig. 1). As a result, phospho-transfer from BvgS to the response regulator (BvgA) is known to occur in multiple steps in *Bordetella*.[47,49,52] However, the significance and the relative advantage it confers on the bacterium are not well understood. To investigate the significance of the presence of three domains, we performed simulations for systems where BvgS possessed only

one phospho-transfer domain, and compared against the wild-type BvgS. Simulations were performed with two different BvgS mutants. While both mutants possessed only one phospho-transfer domain, in one mutant, BvgS-P could dephosphorylate itself, while it could not in the other mutant. The two mutant BvgS are called BvgS1C and BvgS1C-DP, respectively. All other biochemical parameters of the two mutant systems were kept identical as the wild type.

Our results indicate that in a BvgS1C mutant, there is a qualitative change in the class 1 expression pattern as compared to the wild type. In wild type cells, class 1 expression increased significantly when the cells transitioned from Bvg^+/Bvg^i state to Bvg^- state, whereas in the BvgS1C mutant, the induction occurred as cells transitioned from Bvg^+ to Bvg^i state. Minimal change in expression occurred as cells moved from Bvg^i to Bvg^- state (Fig. 3). In addition, even in the presence of fully inducing conditions (Bvg^+), the BvgS1C architecture was unable to completely switch off class 1 gene expression.

For class 2 genes, the BvgS1C mutant does not exhibit the biphasic expression dynamics with expression signal or time. In fact, the expression only increases or decreases monotonically with increasing or decreasing signal strength. For class 3 genes, the mutant displayed a graded rise in steady state values for transition to Bvg^i or Bvg^+ from a Bvg^- state. The strongest impact on the expression pattern was observed for class 4 genes. In the absence of three components, class 4 genes failed to express. Thus, we note that the overall impact of replacing the three phospho-transfer domains with a single one (while still allowing dephosphorylation) results in a loss of sensitivity of the system to environmental conditions. This manifests itself with qualitatively different expression profiles for the four classes of genes involved in *B. pertussis* pathogenesis.

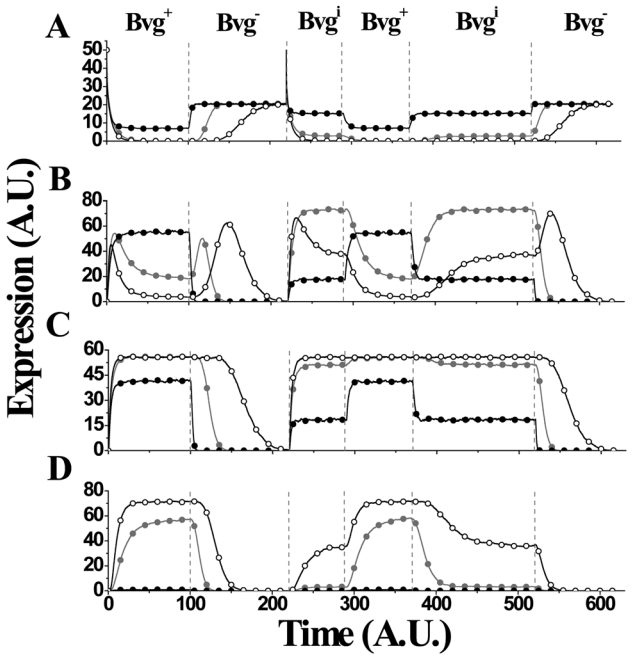

Fig. 3 Dynamics of expression of class 1 (A), class 2 (B), class 3 (C), and class 4 (D) genes in wild-type *Bordetella* (grey), BvgS with a single component (BvgS1C) (black circles), and BvgS with a single component and without dephosphorylation (BvgS1C-DP) (black open circles) in the six transitions between Bvg^-, Bvg^i, and Bvg^+ environments.

The dynamics of the BvgS1C-DP mutant differ from that of the wild type in a different manner. Unlike the BvgS1C mutant, the BvgS1C-DP mutant does not exhibit considerable variation in class 1 expression over the three conditions tested. However, the variation in expression is only in transition from Bvg^i to Bvg^-. There was no difference in expression levels as cells transitioned from Bvg^+ to Bvg^i conditions. The result of loss of dephosphorylation in the BvgS1C-DP mutant restored the biphasic behavior of class 2 gene expression. However, unlike the wild type, the biphasic nature is exhibited over a very narrow range of time (Fig. 3). Similarly, class 3 gene expression in the BvgS1C-DP mutant demonstrates that increased sensitivity of the system to the input signal ensures that transition from the "off" to the "on" state for class 3 genes takes place in the transition from Bvg^- to Bvg^i phase, and there is no change in expression levels between Bvg^i and Bvg^+ phases. Similar results were observed for class 4 gene expression, where removal of the dephosphorylation step effectively meant increasing the sensitivity of the system to the input signal strength. This resulted in faster induction (or slower decay) of genes when transitioned from Bvg^- (or Bvg^+) to Bvg^+ (or Bvg^-).

Dephosphorylation allows for a more graded response to input signals

We next investigated the impact of the dephosphorylation step in the wild type BvgS. To test this, we compared the dynamics of the four classes of genes in wild-type *Bordetella* and a BvgS-mutant (BvgS-DP), where the dephosphorylation step is not permitted. In our simulations, this amounted to setting the rate constant for dephosphorylation equal to zero. Our results show that removal of the dephosphorylation step makes the system more sensitive to the input signal at low values of the input signal (Fig. 4). This results in the entire dynamics of class 1 genes taking place in the Bvg^i to Bvg^- phase transition. By the time cells enter the Bvg^i conditions, class 1 gene expression is completely off. The same behavior was also found for class 2 genes, where removal of dephosphorylation leads to the characteristic biphasic behavior of class 2 gene expression being exhibited in a very narrow window of small values of the input signal strength. This manifests in very slow dynamics of deactivation for class 2 genes in the mutants when the cells are transitioned from Bvg^+ to a Bvg^- state.

The removal of dephosphorylation was found to have a strong impact on the deactivation dynamics (when transitioned from Bvg^+ to Bvg^i/Bvg^- or Bvg^i to Bvg^-) of class 3 genes. Because of the increased sensitivity to the input signal, the mutant demonstrated a delayed inactivation as compared to the wild type. The delay in deactivation came at no apparent additional benefit (like faster induction of class 3 genes). A similar trend of increased sensitivity was displayed in the kinetics of class 4 gene expression. Overall, our results show that the dephosphorylation step in BvgS is responsible for de-sensitizing the system to the input variable, and allows the system to impart a more graded expression pattern in response to the input signal strength.

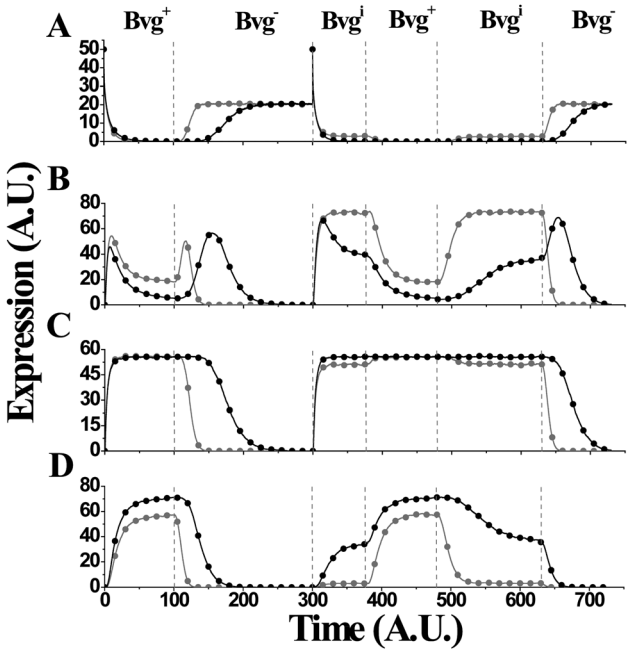

Fig. 4 Comparison of dynamics of class 1 (A), class 2 (B), class 3 (C), and class 4 (D) genes in wild type (grey) and BvgS-DP (BvgS mutant where dephosphorylation is not allowed) (black) in transitions between Bvg^{-}, Bvg^{i}, and Bvg^{+} conditions.

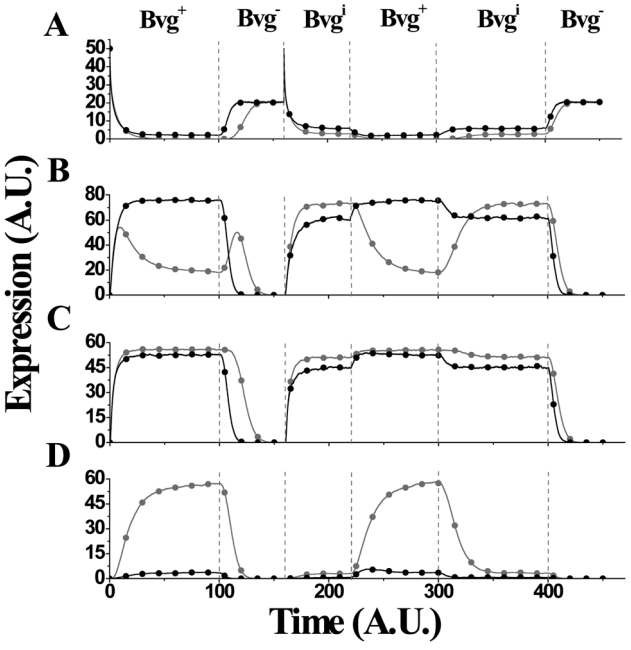

Fig. 5 Comparison of dynamics of class 1 (A), class 2 (B), class 3 (C), and class 4 (D) genes in wild type (grey) and WT-FB (BvgS mutant where positive feedback is not allowed) (black) in transitions between Bvg^{-}, Bvg^{i}, and Bvg^{+} conditions.

We observe that the difference in the expression profile between WT and BvgS-1C is considerable. However, there is minimal difference in the kinetic profile of BvgS-DP and Bvg1C-DP. Based on this, we asked the question: why are the expression profiles of BvgS-DP and BvgS1C-DP so close to each other, when the only difference between them and the pair WT and BvgS1C is the absence of the dephosphorylation step? To answer this, we noted that the flow of phosphate in WT is in several directions: (i) BvgS to BvgA, (ii) BvgA to BvgS, and (iii) BvgS to the environment (dephosphorylation step). In BvgS1C, (ii) and (iii) are eliminated, resulting in a qualitatively different profile between WT and BvgS1C. However, in both BvgS-DP and BvgS1C-DP, step (iii) is eliminated, and consequently the relative significance of step (ii) (eventually leading to dephosphorylation of BvgS) is diminished. Because of this reason, the profiles of BvgS-DP and BvgS1C-DP do not differ qualitatively from each other.

Positive feedback is essential for expression of virulence related genes in *B. pertussis*

Positive feedback has been demonstrated to play an important role in governing gene expression in a number of pathogenic bacteria.[50,59,60] In *Bordetella*, phosphorylated BvgA, in addition to regulating expression of class 1, 2, 3, and 4 promoters, feeds back onto its own promoter and activates expression of the *bvgAS* transcript. The BvgA mediated positive feedback is thought to be critical in controlling expression of virulence genes in the bacterium.[41,61] To test the significance of the positive feedback in the system, we removed the terms equating to the BvgA-P protein activating its promoter. All other terms in the model were kept the same.

On comparing the dynamics of different classes of genes between the wild type and the mutant without the feedback (WT-FB), we conclude that while external signals are important to kick-start the system and control expression of various classes of genes, positive feedback is essential to control the steady-state and long term expression profiles. Our results show that under Bvg^{-} conditions, in the absence of positive feedback, class 1 genes are expressed maximally, and class 2, 3, and 4 genes are not expressed at all (Fig. 5). Moreover, when cells are transitioned from Bvg^{-} to Bvg^{+} state, the change in the input signal leads to the synthesis of some BvgA (and consequently BvgA-P) in the cell. The resulting BvgA-P then represses class 1 expression, leading to a fall in class 1 expression levels. However, in the absence of positive feedback, there is insufficient BvgA in the cell to completely turn off class 1 genes in Bvg^{+} conditions.

In addition, class 2 gene expression exhibits a qualitatively different expression profile in this mutant. Due to reduced levels of BvgA in the cell, class 2 gene expression does not exhibit the biphasic expression characteristic and their expression increases monotonically with signal strength. Hence, we conclude that positive feedback is essential to turn off class 2 gene expression in Bvg^{+} conditions.

Due to the high affinity of class 3 promoters for BvgA, it was expected that class 3 gene expression would not vary between the wild type and the mutant without positive feedback. As expected, our simulations show that class 3 expression remains qualitatively unaltered in this mutant. However, the absence of positive feedback abolishes class 4 expression from the mutant. Similar behaviour regarding virulence gene expression has been observed in *B. pertussis* in an experimental study published in 2007.[41] Hence, our simulations show that positive feedback

plays a critical role in controlling gene expression levels and ensuring the correct timing of expression of each class of genes in *Bordetella*.

Virulence gene expression at a single-cell resolution

Positive feedback has been shown to elicit heterogeneity at a single-cell level.[60] However, the mere presence of positive feedback does not necessarily imply heterogeneity at a single-cell resolution. The regulatory control of *B. pertussis* pathogenesis is under a positive feedback control of the BvgAS two-component system. This control is mediated when phosphorylated BvgA feeds back onto the *bvgA* promoter and activates transcription. Through our model, we tested if the positive feedback encoded in the BvgAS system is sufficient to exhibit a heterogeneous transition from the ''off'' to the ''on'' state, and *vice versa*.

Our simulations demonstrate that at a single-cell resolution, the *bvgAS* regulated genes exhibit a number of qualitative features (Fig. 6 and Fig. S1–S6, ESI†). For clarity, Fig. 6 only includes the time points where heterogeneity is observed. The complete data at all time points evaluated are presented in Fig. S1–S6, ESI.† Class 1 genes exhibit a rheostat-like expression when they are being ''switched off'' by BvgA-P. Here, by rheostat-like expression, we mean that the entire population moves as a single normal curve from lower levels of expression to higher levels, as we go forward in time. However, there is cell-to-cell transient variability as class 1 genes are switched on, upon transition from Bvg^+ to Bvg^- or Bvg^i to Bvg^-. Interestingly, the heterogeneity is observed as the BvgA-mediated positive feedback is switched off. This suggests that, on being transferred from Bvg^+ to Bvg^- conditions, the BvgA amounts inside the cell decrease non-uniformly across the population, leading to heterogeneity at the class 1 gene expression level. This was indeed confirmed from our modeling results (data not shown).

Class 2 and class 4 gene expression levels do not exhibit any qualitative feature at a single-cell resolution. Class 4 gene expression is absent in the absence of positive feedback, and class 2 gene expression exhibits a rheostat-like increase (or decrease) in gene expression. Class 3 gene expression (due to high affinity for BvgA-P) exhibits a switch-like induction in gene expression. There is minimal difference in class 3 expression levels between the Bvg^i and Bvg^+ conditions.

Reverse flow of phosphate results in a faster deactivation dynamics

BvgAS phosphorelay consists of two phosphotransfer steps which are in reverse direction to that described earlier in the text. Specifically, the phosphate group on BvgA can be transferred to the phosphotransfer domain, and the phosphate group on the BvgS's phosphotransfer domain can also be transferred to the receiver domain on BvgS[18] (Fig. 1). This flow is against the direction of activation of BvgA, and hence is likely to impact the dynamics of expression of virulence-associated genes.

To test the role of reversible steps in phosphate transfer, we tested the dynamics of class 1, 2, 3, and 4 genes in wild type and in mutants (BvgS-R) where the reversibility of the phosphate-flow was not permitted (Fig. 7). The impact on the dynamics of gene expression of the virulence-related genes demonstrates that the reversibility in the phosphorelay ensures that upon removal of the activation signal, the bacterium quickly adapts to the new surroundings, and adjusts its gene expression appropriately. Specifically, on removal of the activating signal, BvgA is no longer phosphorylated from BvgS. However, BvgA-P transfers the phosphate group to BvgS, thus effectively reducing the concentration of BvgA-P inside the cell, when it is no longer required for activation of class 2, 3, and 4 genes. This also helps

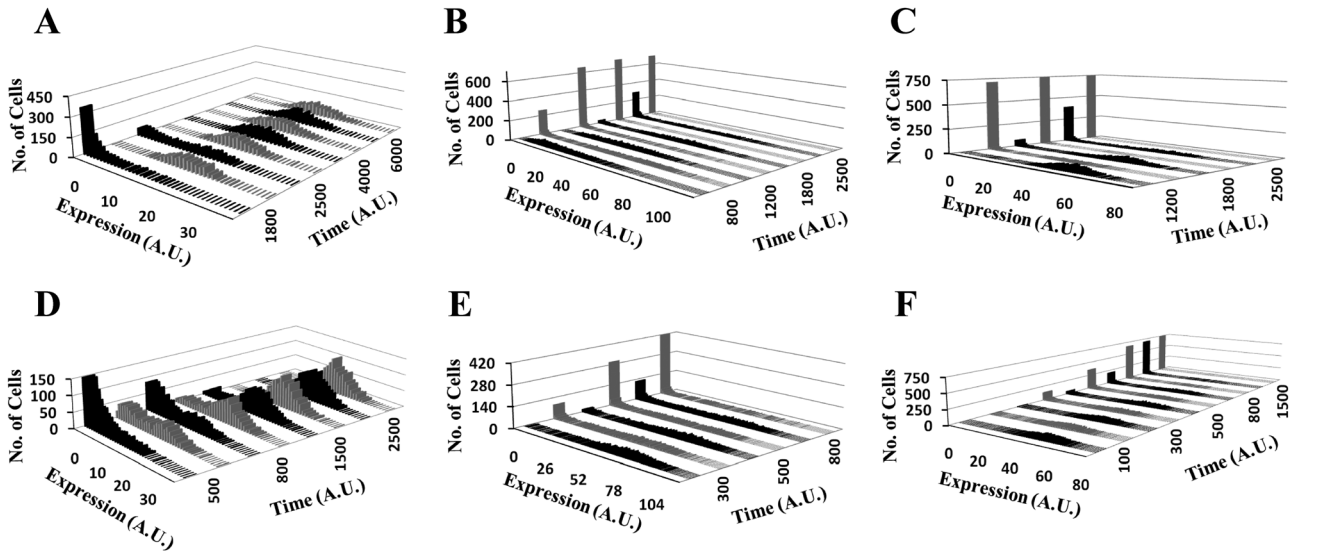

Fig. 6 Expression of *Bordetella* virulence genes at a single-cell resolution. (A–C) Expression of class 1 (panel A), class 2 (panel B), and class 3 (panel C) genes when cells transition from Bvg^+ conditions to Bvg^- conditions. (D–F) Expression of class 1 (panel D), class 2 (panel E), and class 3 (panel F) genes when cells transition from Bvg^i to Bvg^- conditions. Black and gray bars represent expression in WT and mutant (where positive feedback is not allowed) strains respectively. For clarity, only those time points where heterogeneity is most clearly visible are represented here. For all time points, please see Fig. S1–S6, ESI.†

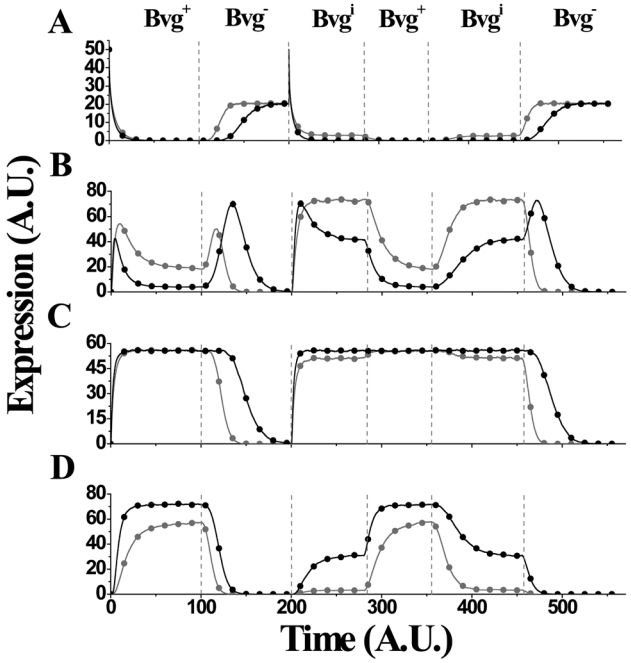

Fig. 7 Comparison of dynamics of class 1 (A), class 2 (B), class 3 (C), and class 4 (D) genes in wild type (grey) and a mutant where reversible phosphorylation is not allowed (BvgS-R) (black) in transitions between Bvg^{-}, Bvg^{i} and Bvg^{+} conditions.

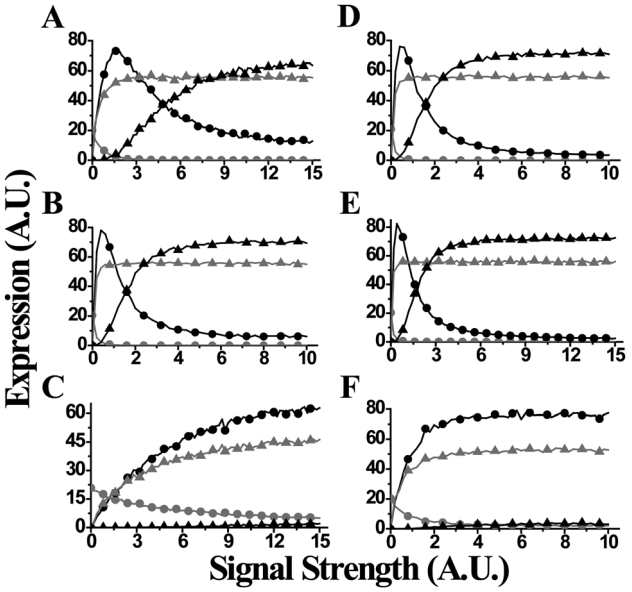

Fig. 8 Steady state analysis of class 1 (grey circles), class 2 (black circles), class 3 (grey triangles), and class 4 (black triangles) genes. The six panels are as follows: (A) wild type, (B) BvgS-DP, (C) BvgS1C, (D) BvgS1C-DP, (E) BvgS-R, and (F) WT-FB.

in faster activation of class 1 genes in the mutant as compared to the wild type.

We also speculated that a side-effect of this arrangement would be slower activation for the wild type (compared to the mutant) of class 2, 3, and 4 genes during transition from Bvg^{-} to Bvg^{+} state. However, our results show that there is no kinetic effect of activation in class 2 and class 3 gene expression. In addition, there is no kinetic effect of deactivation in class 1 gene expression, upon transition of the cells from Bvg^{-} to Bvg^{+} state. However, this arrangement resulted in a significantly faster activation of class 4 genes as compared to the wild type. This faster activation of class 4 genes, however, eliminated the hierarchy of expression of class 3 and class 4 genes. Thus our results indicate that the reversibility in the BvgAS phosphorelay system is encoded for a faster deactivation of the system from the "on" state to the "off" state. The bacterium is able to achieve this desired objective without altering its activation kinetics in a deleterious manner. In fact, a similar role of reverse phosphate flow in TorS has also been demonstrated in *E. coli*.[62]

Steady state analysis of wild type and mutant strains

In addition to studying the dynamics of gene expression, we were also interested in studying the steady state gene expression values for the virulence related genes in *Bordetella*. To investigate this, we computed steady state expression values for class 1, 2, 3, and 4 genes for the wild type and the mutant strains defined in the study. Since many of our results indicate that the most profound impact of the network topology was to increase its adaptability according to the environmental conditions, we tested the same by comparing the steady state values for different classes under different inducer strength conditions. Our results indicate (Fig. 8) that except for the wild type, no other mutant in this study is able to capture the dynamic features of virulence gene expression. These features include (a) turning expressions on and off at various signal strengths; (b) biphasic behaviour of class 2 gene expression; and (c) hierarchy of expression of different classes of genes. Hence, the BvgAS regulatory architecture is "optimal" for controlling virulence gene expression in *Bordetella*.

Interplay between signal strength and positive feedback controls gene expression

The role of positive feedback has been reported to be amplification of environmental signals.[59] Hence, we speculated that positive feedback acts in conjunction with the environmental signal strength to control gene expression. To test this, we simulated the network for 100 different pairs of values for environmental signal strengths and the positive feedback strength. To vary the environmental signal strength we changed the numerical values of the parameter S, and to change the strength of positive feedback, we changed the values of the parameter k_{11}. Our results show that a complex interplay between the two variables is required for control of gene expression in the four classes.

From our simulations, we see that class 1 and class 3 genes are monotonically responsive to environmental signals, with there being minimal dependence on positive feedback for control of gene expression. This lack of dependence on positive feedback is due to high affinities of the promoters for BvgA-P. However, our simulation results show clearly that a minimum critical strength of positive feedback is required to control expression of class 2 and 4 genes. Class 2 genes, like class 3, have high affinity for BvgA-P. However, a decrease in class 2 gene expression requires that we have above a critical minimum of BvgA inside the cell. For this purpose, a critical strength of positive feedback is essential (Fig. 9). Similarly, class 4 gene expression

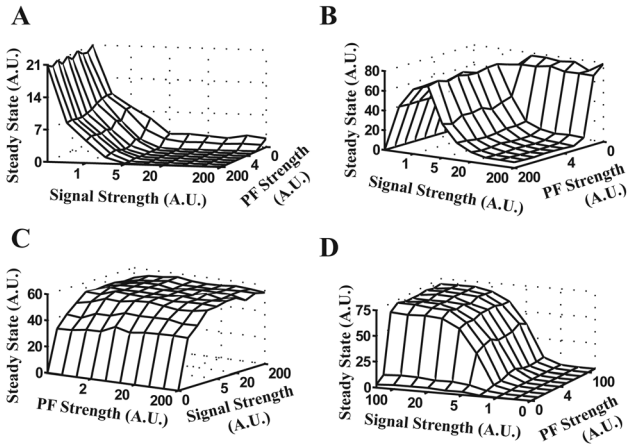

Fig. 9 Steady state as a function of signal strength and positive feedback. Steady state values of class 1 (A), class 2 (B), class 3 (C) and class 4 (D) genes under variable signal strength and positive feedback strength.

takes place only when BvgA levels inside the cell cross a certain minimum. This is achieved through a minimum positive feedback in the system. In addition, the system also requires a minimum signal strength for optimal class 4 expression. Hence, as our simulation results exhibit, virulence gene expression is controlled by the interplay between positive feedback and environmental signal strength. Presumably, this interplay between the two aids the bacterium in identifying precise environmental conditions and launches an appropriate gene expression response.

Sensitivity analysis of the model identifies transfer of the phosphate group as the most sensitive parameter

We next performed a sensitivity analysis on our model, and characterized all model parameters into three groups. The first group included the parameters changing whose values impacted the dynamics minimally. The second group included the parameters a change in whose value only quantitatively changed the dynamics of gene expression. The most important from our perspective was the third group which included parameters a change in whose value would change the expression profile of virulence genes qualitatively. Our analysis shows that there are four critical parameters to which the system is extremely sensitive (data not shown). These include the (a) rate constant of auto-phosphorylation of BvgS, (b) rate constant of transfer of the phosphate group from BvgS to BvgA, (c) rate constant of transfer of the phosphate group from BvgA to BvgS, and (d) rate constant of dephosphorylation of BvgS. Interestingly, our analysis shows that the system is sensitive to (a) and (b) when the bacterium is transferred from Bvg^- to Bvg^+ conditions, and it is sensitive to (c) and (d) when the bacterium is transferred from Bvg^+ to Bvg^- state. These four parameters can be categorized into two pairs. The first pair comprises the rate constant of phosphorylation of BvgS and the rate constant of dephosphorylation of BvgS. The second pair comprises the rate constant of transfer of the phosphate group from BvgS to BvgA and the rate constant of transfer of the phosphate group from BvgA to BvgS. Hence, the two constants in each pair represent the opposite functions in the phosphorelay.

Conclusion

Our simulations indicate that the architecture of the *bvgAS*-regulon is "optimal" for dynamic control of various genes involved in pathogenesis. No other design tested in this study was able to regulate expression of multiple families of genes necessary for infection. Moreover, we demonstrate that the network is controlled by a delicate interplay between feedback and environmental signal strength.

Multiple process control is an emerging theme in bacterial pathogenesis, and control strategies from a number of pathogens have recently been reported.[63,64] While, as reported in this work, the current design outperforms others when compared to its variants, it remains to be seen whether the encoded strategy in the bacterium is the global optimal solution for the control problem. In other words, are there possible regulatory designs which are able to perform the same task as the wild type at a lower cellular cost?

In terms of *Bordetella* pathogenesis, the precise environmental cue that triggers expression remains elusive. The role of environmental cues, growth phase, and general metabolism in controlling gene expression also remains largely unknown.[65,66] Different species of *Bordetella* are known to survive in different environments, and also link gene expression of virulence-related genes with the growth profile. How these critical signals integrate to launch an offensive inside the host cell remains the focus of future studies.

Acknowledgements

The work was funded by the Innovative Young Biotechnologist Award (IYBA) 2010, Department of Biotechnology, Government of India.

References

1 P. A. Cotter and J. F. Miller, in *Principles of Bacterial Pathogenesis*, ed. E. Groisman, Elsevier, 2001, pp. 619–674.
2 J. D. Cherry, *Clin. Infect. Dis.*, 1999, **28**(suppl 2), S112–S117.
3 A. van der Zee, F. Mooi, J. Van Embden and J. Musser, *J. Bacteriol.*, 1997, **179**, 6609–6617.
4 J. M. Musser, E. L. Hewlett, M. S. Peppler and R. K. Selander, *J. Bacteriol.*, 1986, **166**, 230–237.
5 J. Parkhill, M. Sebaihia, A. Preston, L. D. Murphy, N. Thomson, D. E. Harris, M. T. G. Holden, C. M. Churcher, S. D. Bentley, K. L. Mungall, A. M. Cerdeño-Tárraga, L. Temple, K. James, B. Harris, M. A. Quail, M. Achtman, R. Atkin, S. Baker, D. Basham, N. Bason, I. Cherevach, T. Chillingworth, M. Collins, A. Cronin, P. Davis, J. Doggett, T. Feltwell, A. Goble, N. Hamlin, H. Hauser, S. Holroyd, K. Jagels, S. Leather, S. Moule, H. Norberczak, S. O'Neil, D. Ormond, C. Price, E. Rabbinowitsch, S. Rutter, M. Sanders, D. Saunders, K. Seeger, S. Sharp, M. Simmonds, J. Skelton, R. Squares, S. Squares, K. Stevens, L. Unwin, S. Whitehead, B. G. Barrell and D. J. Maskell, *Nat. Genet.*, 2003, **35**, 32–40.

6 J. Cherry and U. Heininger, in *Textbook of Pediatric Infectious Diseases*, ed. R. Feigin and J. Cherry, Saunders, Philadelphia, Pa, 4th edn, 1998, pp. 1423–1440.
7 J. Bordet and O. Gengou, *Ann. Inst. Pasteur*, 1906, **20**, 731–741.
8 S. Mattoo and J. D. Cherry, *Clin. Microbiol. Rev.*, 2005, **18**, 326–382.
9 J. M. Warfel, J. Beren and T. J. Merkel, *J. Infect. Dis.*, 2012, **206**, 902–906.
10 M. H. Yuk, P. A. Cotter and J. F. Miller, *Am. J. Respir. Crit. Care Med.*, 1996, **154**, S150–S154.
11 A. A. Weiss and E. L. Hewlett, *Annu. Rev. Microbiol.*, 1986, **40**, 661–686.
12 T. M. Finn and L. A. Stevens, *Mol. Microbiol.*, 1995, **16**, 625–634.
13 P. B. Cornia, A. L. Hersh, B. A. Lipsky, T. B. Newman and R. Gonzales, *JAMA, J. Am. Med. Assoc.*, 2010, **304**, 890–896.
14 J. E. Godson, *Br. Med. J.*, 1900, **2**, 1310.
15 S. Knapp and J. J. Mekalanos, *J. Bacteriol.*, 1988, **170**, 5059–5066.
16 B. W. Lacey, *J. Hyg.*, 1960, **58**, 57–93.
17 Z. Pusztai and I. Joo, *Ann. Immunol. Hung.*, 1967, **10**, 63–70.
18 P. A. Cotter and A. M. Jones, *Trends Microbiol.*, 2003, **11**, 367–373.
19 P. A. Cotter and V. J. DiRita, *Annu. Rev. Microbiol.*, 2000, **54**, 519–565.
20 A. M. Jones, P. E. Boucher, C. L. Williams, S. Stibitz and P. A. Cotter, *Mol. Microbiol.*, 2005, **58**, 700–713.
21 P. Steffen, S. Goyard and A. Ullmann, *EMBO J.*, 1996, **15**, 102–109.
22 D. T. Beattie, R. Shahin and J. J. Mekalanos, *Infect. Immun.*, 1992, **60**, 571–577.
23 B. J. Akerley, D. M. Monack, S. Falkow and J. F. Miller, *J. Bacteriol.*, 1992, **174**, 980–990.
24 B. J. Akerley and J. F. Miller, *J. Bacteriol.*, 1993, **175**, 3468–3479.
25 R. Deora, *J. Bacteriol.*, 2002, **184**, 6942–6951.
26 C. L. Williams, P. E. Boucher, S. Stibitz and P. A. Cotter, *Mol. Microbiol.*, 2005, **56**, 175–188.
27 K. E. Stockbauer, B. Fuchslocher, J. F. Miller and P. A. Cotter, *Mol. Microbiol.*, 2001, **39**, 65–78.
28 R. Deora, H. J. Bootsma, J. F. Miller and P. A. Cotter, *Mol. Microbiol.*, 2001, **40**, 669–683.
29 D. A. Relman, M. Domenighini, E. Tuomanen, R. Rappuoli and S. Falkow, *Proc. Natl. Acad. Sci. U. S. A.*, 1989, **86**, 2637–2641.
30 F. R. Mooi, W. H. Jansen, H. Brunings, H. Gielen, H. G. van der Heide, H. C. Walvoort and P. A. Guinee, *Microb. Pathog.*, 1992, **12**, 127–135.
31 M. Roberts, N. F. Fairweather, E. Leininger, D. Pickard, E. L. Hewlett, A. Robinson, C. Hayward, G. Dougan and I. G. Charles, *Mol. Microbiol.*, 1991, **5**, 1393–1404.
32 A. Prugnola, B. Aricò, R. Manetti, R. Rappuoli and V. Scarlato, *Microbiology*, 1995, **141**, 2529–2534.
33 V. Scarlato, B. Aricò, A. Prugnola and R. Rappuoli, *EMBO J.*, 1991, **10**, 3971–3975.
34 E. L. Hewlett, V. M. Gordon, J. D. McCaffery, W. M. Sutherland and M. C. Gray, *J. Biol. Chem.*, 1989, **264**, 19379–19384.
35 M. Pittman, *Rev. Infect. Dis.*, 1979, **1**, 401–412.
36 M. H. Yuk, E. T. Harvill, P. A. Cotter and J. F. Miller, *Mol. Microbiol.*, 2000, **35**, 991–1004.
37 M. H. Yuk, E. T. Harvill and J. F. Miller, *Mol. Microbiol.*, 1998, **28**, 945–959.
38 I. Livey and A. C. Wardlaw, *J. Med. Microbiol.*, 1984, **17**, 91–103.
39 S. Mattoo, A. Foreman-Wykert, P. Cotter and J. Miller, *Front. Biosci.*, 2001, **6**, E168–E186.
40 A. Preston, E. Maxim, E. Toland, E. J. Pishko, E. T. Harvill, M. Caroff and D. J. Maskell, *Mol. Microbiol.*, 2003, **48**, 725–736.
41 C. L. Williams and P. A. Cotter, *J. Bacteriol.*, 2007, **189**, 1974–1982.
42 T. L. Nicholson, A. M. Buboltz, E. T. Harvill and S. L. Brockmeier, *Infect. Immun.*, 2009, **77**, 4221–4231.
43 D. T. Gillespie, *J. Phys. Chem.*, 1977, **81**, 2340–2361.
44 D. T. Gillespie, *J. Comput. Phys.*, 1976, **22**, 403–434.
45 C. R. Roy, J. F. Miller and S. Falkow, *J. Bacteriol.*, 1989, **171**, 6338–6344.
46 J. Miller, C. Roy and S. Falkow, *J. Bacteriol.*, 1989, **171**, 6345–6348.
47 M. A. Uhl and J. F. Miller, *EMBO J.*, 1996, **15**, 1028–1036.
48 C. R. Roy and S. Falkow, *J. Bacteriol.*, 1991, **173**, 2385–2392.
49 M. A. Uhl and J. F. Miller, *Proc. Natl. Acad. Sci. U. S. A.*, 1994, **91**, 1163–1167.
50 V. Scarlato, A. Prugnola, B. Aricó and R. Rappuoli, *Proc. Natl. Acad. Sci. U. S. A.*, 1990, **87**, 10067.
51 P. Boucher, F. Menozzi and C. Locht, *J. Mol. Biol.*, 1994, **241**, 363–377.
52 D. Beier, B. Schwarz, T. M. Fuchs and R. Gross, *J. Mol. Biol.*, 1995, **248**, 596–610.
53 R. Gross and N. Carbonetti, *Zentralbl. Bakteriol.*, 1993, **49**, 222–231.
54 D. Beier, T. Fuchs, H. Graeff-Wohlleben and R. Gross, *Microbiologia*, 1996, **12**, 185–196.
55 S. Kinnear, R. Marques and N. Carbonetti, *Infect. Immun.*, 2001, **69**, 1983–1993.
56 A. Smith, C. A. Guzmán and M. Walker, *FEMS Microbiol. Rev.*, 2001, **25**, 309–333.
57 T. Merkel, S. Stibitz, J. Keith, M. Leef and R. Shahini, *Infect. Immun.*, 1998, **66**, 4367–4373.
58 E. J. Capra and M. T. Laub, *Annu. Rev. Microbiol.*, 2012, **66**, 325–347.
59 S. Saini, J. R. Ellermeier, J. M. Slauch and C. V Rao, *PLoS Pathog.*, 2010, **6**, e1001025.
60 D. Shin, E.-J. Lee, H. Huang and E. A. Groisman, *Science*, 2006, **314**, 1607–1609.
61 C. R. Roy, J. F. Miller and S. Falkow, *Proc. Natl. Acad. Sci. U. S. A.*, 1990, **87**, 3763–3767.
62 M. Ansaldi, C. Jourlin-castelli, M. Lepelletier, L. Théraulaz, V. Méjean, C. Jourlin-castelli and L. D. C. Bacte, *J. Bacteriol.*, 2001, **183**, 2691–2695.
63 J. L. Mellies, A. M. S. Barron and A. M. Carmona, *Infect. Immun.*, 2007, **75**, 4199–4210.
64 S. Saini, J. M. Slauch, P. D. Aldridge and C. V. Rao, *J. Bacteriol.*, 2010, **192**, 5767–5777.
65 M. M. Brinig, C. A. Cummings, G. N. Sanden, P. Stefanelli, A. Lawrence and D. A. Relman, *J. Bacteriol.*, 2006, **188**, 2375–2382.
66 M. M. Nakamura, S.-Y. Liew, C. A. Cummings, M. M. Brinig, C. Dieterich and D. A. Relman, *Infect. Immun.*, 2006, **74**, 5537–5548.

